

## Electrostatic Force Theory for a Molecule and Interacting Molecules. II. Shapes of the Ground- and Excited-State Molecules

Hiroshi Nakatsuji

Contribution from the Department of Hydrocarbon Chemistry,  
Faculty of Engineering, Kyoto University, Kyoto, Japan.

Received May 8, 1972

**Abstract:** The electrostatic force (ESF) theory developed in the previous paper was successfully applied to the shapes of both the ground and the excited states of a wide variety of molecules of the types  $AH_2$ ,  $AH_3$ ,  $HAX$ ,  $XHY$ ,  $H_2AX$ , and  $XAY$ . Indeed, among these molecules for which the shapes are known experimentally, no exceptions were found missing from this theory. In these, simple molecular orbitals were used in order to obtain qualitative features of electron density distributions. The relative importance of the atomic dipole (AD), exchange (EC), and gross charge (GC) forces and the various important effects on these forces (e.g., the central atom effect, the central symmetry effect, and the inductive substituent effects on the AD and EC forces; etc.) summarized previously were shown very useful in understanding not only the trends within a type of molecule but also the relations among different types of molecules. Similar to the Walsh rule, the ESF theory also correlates shapes of molecules with the number of valence electrons, although the basic approaches are quite different between these two theories. Moreover, the ESF theory was able to give simple accounts even to the shapes of the molecules for which other theories of molecular structure such as the Walsh rule, the valence-shell electron-pair repulsion (VSEPR) theory, and the second-order Jahn-Teller (SOJT) theory found difficult to give straightforward explanations.

Many models have been developed for molecular geometries, especially for the shapes of molecules. In 1953, Walsh<sup>1</sup> gave the "orbital correlation diagrams" which interconnect the number of valence electrons and the shapes of molecules in their ground and lower excited states. Although his rule is very successful,<sup>2</sup> no firm theoretical bases are yet found for the simple effective one-electron energy.<sup>3</sup> The valence-shell electron-pair repulsion (VSEPR) theory<sup>4,5</sup> chiefly owed to Gillespie and Nyholm is very pictorial and successful, although restrictive only to the ground-state molecules and weak in its theoretical foundations. In conjunction with the Walsh rule, a device to allow the theory semiquantitative predictions of bond angles has recently been reported.<sup>6</sup> The second-order<sup>7</sup> (pseudo-<sup>5</sup>) Jahn-Teller (SOJT) theory developed by Bader,<sup>8</sup> Bartell,<sup>5</sup> Pearson,<sup>7</sup> and Salem<sup>9</sup>

gave the symmetry rule of molecular structure. Similar formulation can also give a theoretical foundation of the symmetry rule of reaction path,<sup>9,10</sup> such as the well-known Woodward-Hoffmann rule.<sup>11</sup>

Aside from the details, the above three theories give, of course, similar and generally correct predictions and so should be different side views of physical reality. Theoretically, the Walsh and SOJT theories are based on the molecular orbital (MO) concept, and the VSEPR theory is close to the valence bond and localized orbital concepts.<sup>12</sup>

Although the above three theories are all based on the *energetic* considerations, the problems of molecular structure can also be studied by considering the *forces* acting on the constituent nuclei. In the previous paper,<sup>13</sup> the *electrostatic force (ESF) theory* in which chemical phenomena are studied through the force concept is presented on the basis of the electrostatic theorem of Hellmann and Feynman.<sup>14</sup> Taking ad-

(1) A. D. Walsh, *J. Chem. Soc.*, 2260, 2266, 2288, 2296, 2301, 2306, 2321 (1953).

(2) B. M. Gimarc, *J. Amer. Chem. Soc.*, **92**, 266 (1970); **93**, 593, 815 (1971).

(3) C. A. Coulson and B. M. Deb, *Int. J. Quantum Chem.*, **5**, 411 (1971), and references cited therein.

(4) (a) N. V. Sidgwick and H. M. Powell, *Proc. Roy. Soc., Ser. A*, **176**, 153 (1940); (b) C. E. Mellish and J. E. Linnett, *Trans. Faraday Soc.*, **50**, 657 (1954); (c) R. J. Gillespie and R. S. Nyholm, *Quart. Rev., Chem. Soc.*, **11**, 339 (1957); (d) R. J. Gillespie, *J. Chem. Educ.*, **40**, 295 (1963); (e) H. A. Bent, *ibid.*, **40**, 446, 523 (1963); **45**, 768 (1968).

(5) L. S. Bartell, *ibid.*, **45**, 754 (1968).

(6) (a) Y. Takahata, G. W. Schnuelle, and R. G. Parr, *J. Amer. Chem. Soc.*, **93**, 784 (1971); (b) H. B. Thompson, *ibid.*, **93**, 4609 (1971).

(7) R. G. Pearson, *ibid.*, **91**, 1252, 4947 (1969); *J. Chem. Phys.*, **52**, 2167 (1970); **53**, 2986 (1970); *Chem. Phys. Lett.*, **10**, 31 (1971).

(8) R. F. W. Bader, *Mol. Phys.*, **3**, 137 (1960); *Can. J. Chem.*, **40**, 1164 (1962).

(9) L. Salem, *Chem. Phys. Lett.*, **3**, 99 (1969).

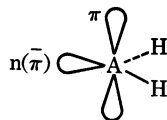
(10) (a) L. Salem and J. S. Wright, *J. Amer. Chem. Soc.*, **91**, 5948 (1969); (b) R. G. Pearson, *Theor. Chim. Acta*, **16**, 107 (1970); *Accounts Chem. Res.*, **4**, 152 (1971).

(11) (a) R. B. Woodward and R. Hoffmann, *Angew. Chem.*, **81**, 797 (1969); "The Conservation of Orbital Symmetry," Academic Press, New York, N. Y., 1969, and their preceding papers cited therein; (b) K. Fukui, "Theory of Orientation and Stereoselection," Springer-Verlag, Heidelberg, 1970.

(12) (a) C. Edmiston and K. Ruendenberg, *Rev. Mod. Phys.*, **35**, 457 (1963); (b) L. C. Allen, *Theor. Chim. Acta*, **24**, 117 (1972).

(13) H. Nakatsuji, *J. Amer. Chem. Soc.*, **95**, 345 (1973), preceding paper which is called paper I.

(14) (a) H. Hellmann, "Einführung in die Quantenchemie," Deuticke, Leipzig, 1937; R. P. Feynman, *Phys. Rev.*, **56**, 340 (1939); see also (b) A. C. Hurley in "Molecular Orbitals in Chemistry, Physics and Biology," P.-O. Löwdin and B. Pullman, Ed., Academic Press, New York, N. Y., 1964, p 161; *Proc. Roy. Soc., Ser. A*, **226**, 170, 179 (1954).

Table I. Shapes of AH<sub>2</sub> Molecules

Shape	Occupation No. of Orbital <sup>a</sup>			—AH <sub>2</sub> <sup>b</sup>
	n( $\bar{\pi}$ )	$\pi$	Rydberg	
Linear	0	0	0 or 1	BeH <sub>2</sub> <sup>+</sup> , BeH <sub>2</sub> , <sup>c</sup> BH <sub>2</sub> <sup>+</sup> , <sup>c</sup> <sup>+</sup> BH <sub>2</sub> , <sup>+</sup> AlH <sub>2</sub>
Bent	1	0	0	BH <sub>2</sub> (131°), AlH <sub>2</sub> (119°)
Bent	1	1	0	CH <sub>2</sub> ( <sup>3</sup> Σ <sub>g</sub> <sup>-</sup> , 136°) <sup>d</sup>
Bent	1	2	0	*NH <sub>2</sub> (144°), *PH <sub>2</sub> (123.1°)
Bent	2	0	0	CH <sub>2</sub> ( <sup>1</sup> A <sub>1</sub> , 102.4°), BH <sub>2</sub> <sup>-</sup> [102°], <sup>e</sup> NH <sub>2</sub> <sup>+</sup> [120°], <sup>c</sup> SiH <sub>2</sub> (...)
Bent	2	1	0 or 1	NH <sub>2</sub> (103.4°), PH <sub>2</sub> (91.5°), <sup>+</sup> OH <sub>2</sub> (106.9°)
Bent	2	2	0	OH <sub>2</sub> (105.2°), SH <sub>2</sub> (92.2°), SeH <sub>2</sub> (91°), TeH <sub>2</sub> (90.25°), NH <sub>2</sub> <sup>-</sup> (104°)

<sup>a</sup> See above figure. <sup>b</sup> Values in ( ) and [ ] mean the apex angles obtained experimentally and from *ab initio* calculations, respectively. The experimental values are cited from ref 15 and 16. The asterisk and double dagger mean respectively the n→π\* and Rydberg excited states. <sup>c</sup> S. D. Peyerimhoff, R. J. Buenker, and L. C. Allen, *J. Chem. Phys.*, **45**, 734 (1966). <sup>d</sup> G. Herzberg and J. W. C. Johns, *ibid.*, **54**, 2276 (1971). <sup>e</sup> L. M. Sachs, M. Geller, and J. J. Kaufman, *ibid.*, **52**, 974 (1970).

vantage of the physical simplicity and visuality of this theorem, we derived three pictorial concepts such as the atomic dipole (AD), exchange (EC), and gross charge (GC) forces. The AD force represents the attraction between the concerned nucleus A and the center of gravity of the polarized electron distribution belonging to the AO's of atom A. The EC force represents the attraction between nucleus A and the electron distribution piled up in the region between nucleus A and its neighboring atom B through electron exchange. The GC force represents the electrostatic interaction between nucleus A and the gross charge on atom B. In the problems of molecular structure, the relative importances of these forces are

$$\text{AD force} > \text{EC force (triple} > \text{double} > \text{single bond)} \gg \text{GC force} \quad (1)$$

where the EC force depends on bond multiplicity. The AD force is especially important for lone-pair electrons. For molecular shape, the AD force operates to make the molecule nonplanar and the EC force as a main restoring force to planar structure. Note that for hydrogen atoms, the AD force is small. The balancing of these AD, EC, and GC forces determines the molecular structure. In order to extend the applicability of the ESF theory to a wide variety of molecules, the influences on these forces induced by the changes of atom A and substituent B are studied and some regular features are deduced: the central atom effect, the central symmetry effect, and the inductive substituent effect on the AD and EC forces, etc. The change in these forces following the change in electronic structure (*e.g.*, by electron excitation, ionization, electron attachment, etc.) is also discussed. Especially from these, a simple qualitative measure of shapes is obtained for usual molecules (Figure 7 of paper I). For some illustrative examples, the conceptual utility of the ESF theory has been proven in predicting the shapes of molecules in both the ground and excited states and in understanding chemical reactions and the structures of products.

In the present paper, we will show more fully how well the ESF theory works in predicting the shapes of

a wide variety of molecules represented by AH<sub>2</sub>, AH<sub>3</sub>, HAX, XHY, H<sub>2</sub>AX, and XAY in their ground and excited states.<sup>15,16</sup> For example, the present theory interconnects the number of valence electrons and the shapes of molecules from an utterly different standpoint than the Walsh rule. Moreover, we will show that the present ESF theory is able to give simple accounts even to the shapes of the molecules for which other theories of molecular structure such as the Walsh rule, the VSEPR theory, and the SOJT theory found difficult to give straightforward explanations.

**AH<sub>2</sub> Molecules.** The shapes of AH<sub>2</sub> molecules in their ground and excited states are summarized in Table I, where the number shown in the second column is the occupation number of the  $\bar{\pi}$  MO in linear structure (in bent configuration, this MO becomes the n orbital).<sup>17</sup> In AH<sub>2</sub> molecules this number coincides with  $D(p_{\bar{\pi}A})$ , the density of electrons in the  $p_{\bar{\pi}}$  AO of atom A in linear configuration, which was defined in Figure 7 of paper I. We refer to it by  $N(n(\bar{\pi}))$  in this section. The third and fourth columns give also the occupation number of the  $\pi$  and Rydberg orbitals, which are (approximately) symmetric with respect to the central nucleus A. The asterisk and double dagger mean that the molecules are in the n→π\* and Rydberg excited states, respectively. The values shown in ( ) and [ ] are the apex angles obtained experimentally and from *ab initio* calculations, respectively.

As expected from Figure 7 of paper I, when  $N(n(\bar{\pi})) = 0$ , the geometry is linear, while when  $N(n(\bar{\pi})) = 1$  or 2, it is bent. This is due to the increase in the AD force exerted on atom A with increasing  $N(n(\bar{\pi}))$ . Among similar molecules, the extent of bending increases as  $N(n(\bar{\pi}))$  increases: BH<sub>2</sub><sup>+</sup>(180°), <sup>+</sup>BH<sub>2</sub>(180°) → BH<sub>2</sub>(131°) → BH<sub>2</sub><sup>-</sup>[102°]; <sup>+</sup>AlH<sub>2</sub>(180°) → AlH<sub>2</sub>(119°); CH<sub>2</sub>(<sup>3</sup>Σ<sub>g</sub><sup>-</sup>, 136°) → CH<sub>2</sub>(<sup>1</sup>A<sub>1</sub>, 102.4°); \*NH<sub>2</sub>(144°) → NH<sub>2</sub><sup>+</sup>[120°], NH<sub>2</sub>(103.4°), NH<sub>2</sub><sup>-</sup>(104°); \*PH<sub>2</sub>(123.1°) → PH<sub>2</sub>(91.5°). Moreover, the experi-

(15) G. Herzberg, "Molecular Spectra and Molecular Structure. III. Electronic Spectra and Electronic Structure of Polyatomic Molecules," Van Nostrand, Princeton, N. J., 1965.

(16) L. E. Sutton, Ed., *Chem. Soc., Spec. Publ.*, No. 11 (1958); No. 18 (1965).

(17) For triatomic molecules, π and  $\bar{\pi}$  MO's are degenerate in linear structure but split by bending motion. Throughout this paper, we assume that the bending motion occurs on the  $\bar{\pi}$  plane.

mental apex angles shown in Table I can be grouped with respect to  $N(n(\bar{\pi}))$ ; when  $N(n(\bar{\pi})) = 0$ , the apex angle is  $180^\circ$ , when  $N(n(\bar{\pi})) = 1$ , it is  $119\text{--}144^\circ$  (mean value,  $131^\circ$ ), and when  $N(n(\bar{\pi})) = 2$ , it is  $90\text{--}107^\circ$  (mean value,  $98^\circ$ ). In spite of the considerable changes of the central atom A, the constancy in the apex angle is remarkable in each group. This is due to the fact that the relative importance of the AD and EC forces is approximately constant in each group (see Table I, paper I). Since the AD force is more important than the EC force (eq 1), the apex angles of all the molecules with  $N(n(\bar{\pi})) = 2$  are considerably less than  $120^\circ$ .

Since electrons in  $\pi$  and Rydberg orbitals exert no force on atom A by symmetry, they are unimportant for shapes:  $\text{NH}_2(103.4^\circ)$ ,  $\text{NH}_2^-(104^\circ)$ ;  $\text{OH}_2(105.2^\circ)$ ,  $^\pm\text{OH}_2(106.9^\circ)$ . From the central atom effect,<sup>13</sup> the following sequences in apex angles are reasonable:  $\text{BH}_2(131^\circ) > \text{AlH}_2(119^\circ)$ ,  $^*\text{NH}_2(144^\circ) > ^*\text{PH}_2(123.1^\circ)$ ,  $\text{NH}_2(103.4^\circ) > \text{PH}_2(91.5^\circ)$ , and  $\text{OH}_2(105.2^\circ) > \text{SH}_2(92.2^\circ) > \text{SeH}_2(91^\circ) > \text{TeH}_2(90.25^\circ)$ . Note that the marked differences are seen between the first- and second-row elements.

Although all the features of Table I are thus understood from the ESF theory, an exception is there which cannot be explained by the pictorial concept given in paper I. That is the structure of  $\text{LiH}_2^+$ , which is predicted to be bent by the *ab initio* SCF calculations.<sup>18,19</sup> Since in  $\text{LiH}_2^+$  only two valence electrons are there in the framework of three positively charged nuclei (or cores), it may be erroneous to image a "bond" between Li and H, which leads to the EC forces on the Li nucleus resulting in a linear structure. But, perhaps in this extreme system, the electron cloud will more effectively shield the three bare nuclei if it is crowded about the center of the triangular nuclear framework. This may also hold for  $\text{H}_3^+$  and  $\text{Li}_3^+$ .<sup>18-21</sup> The original Walsh rule predicted  $\text{LiH}_2^+$  to be linear,<sup>1</sup> although a modification has recently been made in a rather *ad hoc* manner.<sup>2</sup> However, in the present ESF theory, we can always go back to the fundamental equation (eq 1 or 5, paper I) without any change of the basic concept. Then, it is interesting whether the forces calculated from the *ab initio* charge distributions of  $\text{LiH}_2^+$  can predict bent structures as their energetics did.<sup>18,19</sup> Actually, the Ray's wave functions<sup>19</sup> should predict  $\text{LiH}_2^+$  and  $\text{Li}_3^+$  to be bent even from the force treatment, since his floating wave functions satisfy the Hellmann-Feynman theorem.<sup>14b,22</sup>

As in the Walsh rule,<sup>1</sup> the present ESF theory also correlates the shapes of the ground-state  $\text{AH}_2$  molecules with the number of valence electrons. Namely, from the above discussions, if the number of valence electrons is smaller than or equal to four, the molecule will have a linear structure (except two valence electron systems like  $\text{LiH}_2^+$ ), while if it is five to eight, the molecule will be bent. This result agrees with the Walsh rule, although the starting point is essentially different.

The geometries of  $\text{Li}_2\text{O}$ ,  $\text{LiOH}$ ,  $\text{KOH}$ ,  $\text{RbOH}$ , and  $\text{CsOH}$  are very interesting. Although these molecules

are considered to be the derivatives of  $\text{H}_2\text{O}$ , the experimental geometries of  $\text{Li}_2\text{O}$ ,  $\text{KOH}$ ,  $\text{RbOH}$ , and  $\text{CsOH}$  are linear or approximately linear.<sup>23</sup> *Ab initio* SCF calculations<sup>24</sup> also predicted  $\text{Li}_2\text{O}$  and  $\text{LiOH}$  to be linear. However, Buenker and Peyerimhoff<sup>24</sup> showed that the orbital correlation diagrams (not the total energy curves) of  $\text{Li}_2\text{O}$  and  $\text{LiOH}$  did not give the correct molecular shapes because of the highly ionic character of these compounds. The extended Hückel correlation diagram also broke down for these highly ionic compounds.<sup>25</sup> For similar reasons, the SOJT theory also failed in predicting the shapes of these molecules.<sup>7</sup> On the other hand, in the present ESF theory the shapes of these molecules can be treated in two alternative ways. One is to treat these molecules as the derivatives of  $\text{H}_2\text{O}$  by referring to the substituent effects summarized in paper I. The other is to treat these molecules in the framework of HAX and XAY molecules. In this section, we give the first treatment. The latter treatment will be given in the respective sections. Of course, the results of these alternative treatments are consistent.

Since alkali metal is more electropositive than hydrogen and since it has vacant p AO's, it acts as a  $\sigma$ -donating and  $\pi$ -attractive substituent compared with hydrogen. Then, from Table II of paper I, the AD force on oxygen decreases. From the inductive substituent effect, the EC force increases. Although the GC force is small, the positive gross charge on the metal repels the other metal or hydrogen nucleus. Since all of the three forces cooperate to make the apex angle larger than  $\text{H}_2\text{O}$ , it is reasonable if these molecules become linear as an extreme. Moreover, Allen, *et al.*,<sup>25,26</sup> reported from *ab initio* calculations that the electronic structure of  $\text{Li}_2\text{O}$  is almost  $\text{Li}^+\text{O}^{2-}\text{Li}^+$ . Then, the linearity of  $\text{Li}_2\text{O}$  is also understandable from the central symmetry effect on the AD force (section ii-2 of paper I).

**AH<sub>3</sub> Molecules.** The shapes of  $\text{AH}_3$  molecules in their ground and excited states are summarized in Table II. The values shown in the second column are the occupation numbers of the  $\pi$  MO in planar configuration, which coincide in this case with  $D(p_{\pi A})$  defined in Figure 7 of paper I. This orbital becomes the lone-pair orbital in pyramidal configuration. Other notations are the same as those in Table I.

An essential difference between  $\text{AH}_2$  and  $\text{AH}_3$  molecules lies in the number of the EC forces acting on atom A along AH bonds. That is, although only two EC forces are there in  $\text{AH}_2$  molecules, three EC forces are there in  $\text{AH}_3$ . Then, although  $\text{CH}_2(^3\Sigma_g^-)$  is bent (Table I),  $\text{CH}_3$  is planar, notwithstanding that  $D(p_{\pi A}) = 1$  for both. However, since the planar structure of  $\text{CH}_3$  is a result of a rather critical balance of the AD and EC forces,<sup>13</sup> the shape of the  $\text{AH}_3$  molecule is easily affected by the central atom effect, substit-

(18) R. D. Poshusta, J. A. Haugen, and D. F. Zetik, *J. Chem. Phys.*, **51**, 3343 (1969).

(19) N. K. Ray, *ibid.*, **52**, 463 (1970).

(20) B. M. Gimarc, *ibid.*, **53**, 1623 (1970).

(21) See also the discussions given in the section on XHY molecules.

(22) A. A. Frost, *J. Chem. Phys.*, **47**, 3707 (1967).

(23) (a)  $\text{Li}_2\text{O}$ : A. Büchler, J. Stauffer, W. Klemperer, and L. Wharton, *ibid.*, **39**, 2299 (1963); D. White, K. S. Seshadri, D. F. Deves, D. E. Mann, and M. J. Leneusky, *ibid.*, **39**, 2463 (1963); (b)  $\text{KOH}$ ,  $\text{RbOH}$ , and  $\text{CsOH}$ : R. L. Kuczkowski, D. R. Lide, Jr., and L. C. Krisher, *ibid.*, **44**, 3131 (1966); D. R. Lide, Jr., and R. L. Kuczkowski, *ibid.*, **46**, 4768 (1967); N. Acquista, S. Abramowitz, and D. R. Lide, *ibid.*, **49**, 780 (1968); C. Matsumura and D. R. Lide, Jr., *ibid.*, **50**, 71, 3080 (1969).

(24) R. J. Buenker and S. D. Peyerimhoff, *ibid.*, **45**, 3682 (1966).

(25) L. C. Allen and J. D. Russell, *ibid.*, **46**, 1029 (1967).

(26) J. E. Liebman and L. C. Allen, quoted by Allen in ref 12b.

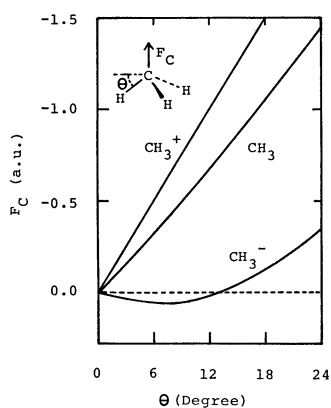


Figure 1. Forces acting on carbon nuclei in  $\text{CH}_3^+$ ,  $\text{CH}_3$ , and  $\text{CH}_3^-$  calculated from the INDO electron distributions.

Table II. Shapes of  $\text{AH}_3$  Molecules

Shape	Occupation No. of $\pi$ orbital	$\text{AH}_3^a$
Planar	0	$\text{CH}_3^+, ^b \text{CH}_3, \text{BH}_3, ^c \text{BeH}_3^-$
Planar	1	$\text{CH}_3, \text{BH}_3^-, ^d \text{NH}_3^+, ^e \text{NH}_3, ^f \text{PH}_3$
Pyramidal	1	$\text{SiH}_3(113.5^\circ), ^g \text{GeH}_3(115^\circ), ^g \text{SnH}_3(117^\circ)$
Pyramidal	2	$\text{CH}_3^-(\text{---}), ^h \text{NH}_3(107.8^\circ), \text{PH}_3(93.3^\circ), \text{AsH}_3(92^\circ), \text{OH}_3^+(117^\circ)$

<sup>a</sup> The double dagger means that the molecule is in the Rydberg excited state. The experimental HAH angles are cited from ref 15 except those specially noted. <sup>b</sup> Theoretical value, ref 31. <sup>c</sup> Theoretical value, ref 31a. <sup>d</sup> M. C. R. Symons and H. W. Wardale, *Chem. Commun.*, 758 (1967); M. C. R. Symons, *Nature (London)*, **222**, 1123 (1969). <sup>e</sup> T. Cole, *J. Chem. Phys.*, **35**, 1169 (1961). <sup>f</sup> W. L. Smith, and P. A. Warsop, *Trans. Faraday Soc.*, **64**, 1165 (1968). <sup>g</sup> Reference 27. <sup>h</sup> C. Bugg, R. Desiderato, and R. L. Sass, *J. Amer. Chem. Soc.*, **86**, 3157 (1964).

uent effect, etc. For example,  $\text{SiH}_3$ ,  $\text{GeH}_3$ , and  $\text{SnH}_3$ <sup>27</sup> and fluoromethyl radicals<sup>28</sup> become pyramidal.<sup>13</sup>

For the prototype molecules  $\text{CH}_3^+$ ,  $\text{CH}_3$ , and  $\text{CH}_3^-$ , detailed discussions are given in paper I about the roles of the AD, EC, and GC forces in determining their molecular shapes. Here, we actually calculated the forces acting on the carbon atom from the INDO charge distributions.<sup>29</sup> The results are illustrated in Figure 1. In these, Slater orbitals are assumed for the basic AO's and eq 5 of paper I (not the approximate eq 13) is used. All the integrals up to three center are rigorously calculated by the Gaussian expansion of the Slater-type orbitals.<sup>30</sup> Figure 1 predicts that  $\text{CH}_3^+$  and  $\text{CH}_3$  should be planar and  $\text{CH}_3^-$  pyramidal with the out-of-plane angle  $\theta$  to be  $\sim 12^\circ$ . The resultant shapes agree with the previous predictions given in paper I and with the more rigorous *ab initio* calculations<sup>31</sup> and the experiments.<sup>15,16,32,33</sup>

(27) R. L. Morehouse, J. J. Christiansen, and W. Gordy, *J. Chem. Phys.*, **45**, 1751 (1966); G. S. Jackel, J. J. Christiansen, and W. Gordy, *ibid.*, **47**, 4274 (1967); G. S. Jackel and W. Gordy, *Phys. Rev.*, **176**, 443 (1968); see also, P. J. Krusic and J. K. Kochi, *J. Amer. Chem. Soc.*, **91**, 3938 (1969).

(28) R. W. Fessenden and R. H. Schuler, *J. Chem. Phys.*, **43**, 2704 (1965).

(29) J. A. Pople, D. L. Beveridge, and P. A. Dobosh, *ibid.*, **47**, 2026 (1967); J. A. Pople and D. L. Beveridge, "Approximate Molecular Orbital Theory," McGraw-Hill, New York, N. Y., 1970.

(30) K. O-ohata, H. Taketa, and S. Huzinaga, *J. Phys. Soc. Jap.*, **21**, 2306 (1966); R. F. Stewart, *J. Chem. Phys.*, **52**, 431 (1970); see also, H. Taketa, S. Huzinaga, and K. O-ohata, *J. Phys. Soc. Jap.*, **21**, 2313 (1966).

(31) (a) S. D. Peyerimhoff, R. J. Buenker, and L. C. Allen, *J. Chem. Phys.*, **45**, 734 (1966); (b) G. V. Bünau, G. Diercksen, and H. Preuss,

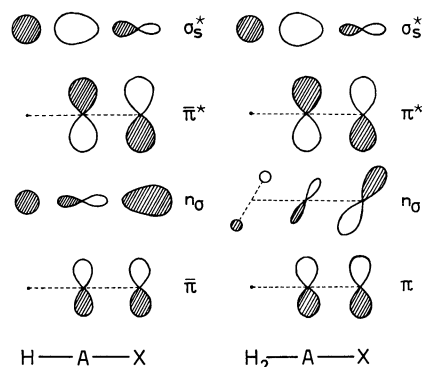


Figure 2. Illustration of the MO density distributions in HAX and  $\text{H}_2\text{AX}$  molecules. A hatch is made in order to show the bonding and antibonding characters of the MO's; see also ref 36.

The Rydberg excited states of  $\text{CH}_3$ ,  $\text{NH}_3$ , and  $\text{PH}_3$  are all planar. Since these Rydberg orbitals are approximately symmetric about the central nucleus,  $^{\ddagger}\text{CH}_3$  is planar<sup>15</sup> as  $\text{CH}_3^+$  is, and  $^{\ddagger}\text{NH}_3$ <sup>15</sup> and  $^{\ddagger}\text{PH}_3$ <sup>34</sup> are planar as  $\text{NH}_3^+$  is.<sup>35</sup>

A valence-bond calculation of the hypothetical molecule  $\text{LiH}_3^+$  indicated that this three-valence-electron ion should be Y shaped.<sup>18</sup> Since the electronic structure of  $\text{LiH}_3^+$  in the  $D_{3h}$  structure is degenerate, the Y-shaped geometry is a consequence of the first-order Jahn-Teller effect.

As in the Walsh rule,<sup>1</sup> the present ESF theory also correlates the shapes of the ground-state  $\text{AH}_3$  molecules with the number of valence electrons. If the number of valence electrons is three to five, the molecule will be Y shaped, due to the first-order Jahn-Teller effect. If it is six, the molecule will be planar, but if it is seven, the shape will be planar or pyramidal, depending on the central atom effect and the substituent effect on the AD force. If it is eight, the molecule will be pyramidal.

**HAX Molecules.** The shapes of HAX molecules in their ground and excited states are summarized in Table III, where the asterisk means that the molecule is in the excited state. For the linear configuration of HAX molecules, the density distributions of the  $\pi$  ( $\bar{\pi}$ ),  $n_\sigma$ ,  $\pi^*$  ( $\bar{\pi}^*$ ), and  $\sigma_s^*$  MO's are illustrated in Figure 2.  $\pi$  ( $\bar{\pi}$ ) and  $\pi^*$  ( $\bar{\pi}^*$ ) MO's are the bonding and antibonding orbitals composed of the two  $p_\pi$  AO's centered on A and X atoms.<sup>36</sup>  $n_\sigma$  MO is the  $\sigma$ -bonding orbital between A and H and almost lone-pair orbital on atom X.  $\sigma_s^*$  MO is the  $\sigma_{\text{A-SH}}$  and  $\sigma_{\text{A-P}_\sigma\text{X}}$  antibonding orbital in which the  $\sigma_{\text{A}}$  orbital is mainly composed of the  $s_{\text{A}}$  AO. Degenerate  $\pi$  and  $\bar{\pi}$  MO's in linear

*Int. J. Quantum Chem.*, **1**, 645 (1967); (c) K. Morokuma, L. Pedersen, and M. Karplus, *J. Chem. Phys.*, **48**, 4801 (1968); (d) R. E. Kari and I. G. Csizmadia, *ibid.*, **50**, 1443 (1969).

(32) W. L. S. Andrews and G. C. Pimentel, *ibid.*, **44**, 2527 (1966); D. E. Milligan and M. E. Jacox, *ibid.*, **47**, 5146 (1967).

(33) C. Bugg, R. Desiderato, and R. L. Sass, *J. Amer. Chem. Soc.*, **86**, 3157 (1964).

(34) W. L. Smith and P. A. Warsop, *Trans. Faraday Soc.*, **64**, 1165 (1968).

(35) T. Cole, *J. Chem. Phys.*, **35**, 1169 (1961).

(36) The bonding and antibonding orbitals are written as  $\varphi_b = (p_{\bar{\pi}\text{A}} + p_{\bar{\pi}\text{X}})/(2 + 2S)^{1/2}$  and  $\varphi_a = (p_{\bar{\pi}\text{A}} - p_{\bar{\pi}\text{X}})/(2 - 2S)^{1/2}$  if the A-X bond is homopolar. From the square of these orbitals, the MO density distributions shown in Figure 2 is drawn. Note that the contributions to  $D(p_{\bar{\pi}\text{A}})$  from doubly occupied bonding and antibonding orbitals are  $1/(1 + S) \approx 0.8$  and  $1/(1 - S) \approx 1.4$  ( $S \approx 0.3$ ), respectively, and that the contribution to the bond order between  $p_{\bar{\pi}\text{A}}$  and  $p_{\bar{\pi}\text{X}}$  AO's is negative for the antibonding orbital.

Table III. Shapes of HAX Molecules<sup>a</sup>

Shape	Occupation No. of MO <sup>b</sup>					HAX
	$\sigma_p(\bar{\pi})$	$\pi$	$n_\sigma$	$n(\bar{\pi}^*)$	$\pi^*$	
Linear	2	2	0	0	0	HOLi, <sup>c</sup> HOK, <sup>d</sup> HORb, <sup>d</sup> HOCs <sup>d</sup>
	2	2	2	0	0	HCN, HCP
	2	2	2	0	1	*HCO
Bent	2	2	1	1	0	*HCN (141°)
	2	1	2	1	0	*HCN (125, 114°)
	2	2	2	1	0	HCO (119.5°)
	2	2	2	1	1	*HNO (118.6°), *HCF (127.2°), *HCCI (134°), *HSiCl (116.1°), *HSiBr (116.6°)
	2	2	2	2	0	HNO (108.6°), HPO (104.7°), HCF (101.6°), HCCI (103.4°), HSiCl (102.8°), HSiBr (102.9°)
	2	2	2	2	1	HOO (...), <sup>e</sup> HNF (...), <sup>f</sup> HOF [~100°], <sup>c</sup> HOCl (113°), <sup>g</sup> HOBr (...) <sup>h</sup>

<sup>a</sup> The experimental apex angles are cited from ref 15 except those specially noted. The asterisk means that the molecule is in the excited state. <sup>b</sup> The  $\pi$ ,  $n_\sigma$ , and  $\pi^*$  MO's are approximately unimportant for the bending on the  $\bar{\pi}$  plane; see the text. <sup>c</sup> From *ab initio* calculations, ref 24. <sup>d</sup> Reference 23. <sup>e</sup> D. E. Milligan and M. E. Jacox, *J. Chem. Phys.*, **38**, 2627 (1963). <sup>f</sup> M. E. Jacox and D. E. Milligan, *ibid.*, **46**, 184 (1967). <sup>g</sup> Reference 16. <sup>h</sup> I. Schwager and A. Arkell, *J. Amer. Chem. Soc.*, **89**, 6006 (1967).

structure split into  $\pi$  and  $\sigma_p$  MO's in bent configuration and similarly  $\pi^*$  and  $\bar{\pi}^*$  MO's into  $\pi^*$  and  $n$  MO's;  $\sigma_p$  and  $n$  MO's are the in-plane  $p_{\bar{\pi}}$  bonding orbital and lone-pair orbital on atom A, respectively. The occupation numbers of these MO's are given in Table III. The  $\sigma_s^*$  MO is empty for these molecules.

An essential difference of HAX molecules from  $AH_2$  and  $AH_3$  molecules is the existence of  $\pi$ -type MO's. One of the most important features in Figure 2 is that the (one center) density on  $p_\pi$  ( $p_{\bar{\pi}}$ ) AO's is smaller in bonding  $\pi$  ( $\bar{\pi}$ ) orbitals than in the antibonding  $\pi^*$  ( $\bar{\pi}^*$ ) orbital. The reason is that in the bonding orbital, the electron(s) in the  $p_\pi$  ( $p_{\bar{\pi}}$ ) AO flow(s) into the A-X bond region, but in the antibonding orbital the reverse occurs due to the existence of a node.<sup>36</sup> Therefore, the  $\pi$  bonding between A and X operates to diminish the AD force and to enlarge the EC force. These effects cooperatively favor the linear structure. The effect of  $\pi$  antibonding is reverse that of  $\pi$  bonding and advantageous for the bent structure.<sup>37</sup> The effect of  $\pi$  bonding on the EC force is already given in eq 1.

Although two nonhydrogen atoms are there in HAX molecules, the change in the total electron distribution induced by bending is expected to be larger near A than near H and X, since for H and X the change should be only of the order of magnitude of nonbonded interaction.<sup>38</sup> Then, approximately, we have only to consider the induced forces on atom A by small bending.

Different from the previous sections,  $D(p_{\bar{\pi}A})$  here is noninteger and the sum of contributions from  $\bar{\pi}$  and  $\bar{\pi}^*$  MO's.<sup>36,17</sup>  $\pi$ ,  $\pi^*$ , and  $n_\sigma$  MO's do not contribute to  $D(p_{\bar{\pi}A})$ , but the occupation of  $\pi$  and  $\pi^*$  MO's affects the EC force as stated above. When  $\bar{\pi}$  and  $n_\sigma$  MO's are singly or doubly filled but  $\bar{\pi}^*$  MO is empty,  $D(p_{\bar{\pi}A})$  is less than or nearly equal to  $1/(1+S) \simeq 0.8$ .<sup>36</sup> Then, the shapes are expected to be linear. An increase in the EC force due to the multiple bond character of the A-X bond also favors linear structure. When the  $\bar{\pi}$  MO is filled and  $\bar{\pi}^*$  MO is singly or doubly filled,  $D(p_{\bar{\pi}A})$  becomes considerably larger than

unity<sup>36</sup> and the molecule is expected to be bent. A decrease in the EC force due to the occupation of the antibonding ( $\bar{\pi}^*$  and/or  $\pi^*$ ) orbital also favors a bent structure. These predictions agree completely with experimental shapes of HAX molecules shown in Table III. Note that the structures of HOLi, HOK, HORb, and HOCs are easily understood to be linear.<sup>23</sup> This is in accord with the discussions given in the previous section. Moreover, since all the molecules shown in Table III have filled  $\bar{\pi}$  MO, the shapes of these molecules become more bent with increasing occupation number of  $\bar{\pi}^*$  MO; when it is zero the apex angle is 180°, when it is unity the apex angle is 116–141° (mean value, 124°), and when it is two the apex angle is 100–113° (mean value, 104°). Note that in the last case,  $D(p_{\bar{\pi}A})$  is larger than or equal to 2.0. Then, the apex angle is expected from eq 1 to be less than 120° as it certainly is.

No experimental shapes are known for the molecules where the  $\sigma_s^*$  MO is filled. For these molecules, Figure 7 of paper I can no longer be applicable from the central symmetry effect on the AD force. Then, the shapes of these molecules are expected to be linear again, although  $D(p_{\bar{\pi}A}) \geq 2$ .

From the above discussions, the shapes of the ground-state HAX molecules are correlated with the number of valence electrons. If it is less than or equal to ten, the molecule will be linear, and if it is 11–14, the molecule will be bent, where from 11 to 12 the apex angle will sharply decrease. If it is 16, the molecule will be linear again.

**XHY Molecules.** The geometry of the ions  $FHF^-$ ,  $ClHCl^-$ , and  $BrHBr^-$ , where hydrogen is located between two halogens, has been observed to be linear and symmetric.<sup>39</sup> The shapes and stabilities of these ions were discussed by MO theories.<sup>2,40</sup> From *ab initio* calculations, Dierksen, *et al.*,<sup>41</sup> and Poshusta, *et al.*,<sup>18</sup> have predicted the four-valence-electron ions,

(39) J. A. Ibers, *J. Chem. Phys.*, **40**, 402 (1964); J. C. Evans and G. Y-S. Lo, *J. Phys. Chem.*, **70**, 11 (1966); **71**, 3697 (1967); **73**, 448 (1969).

(40) G. C. Pimentel, *J. Chem. Phys.*, **19**, 446 (1951); J. W. Linnett, *Science*, **167**, 1719 (1970); G. C. Pimentel and R. D. Spratley, *J. Amer. Chem. Soc.*, **85**, 826 (1963); L. C. Allen, R. M. Erdahl, and J. L. Whitten, *ibid.*, **87**, 3769 (1965); P. N. Noble and R. N. Kortzeborn, *J. Chem. Phys.*, **52**, 5375 (1970).

(41) G. Dierksen and H. Preuss, *Int. J. Quantum Chem.*, **1**, 637, 641 (1967); R. Janoschek, G. Dierksen, and H. Preuss, *ibid.*, **2**, 159 (1968).

(37) These effects of the  $\pi$  overlap will be discussed more fully in the succeeding paper of this series in the framework of overlap effect: H. Nakatsuji, *J. Amer. Chem. Soc.*, submitted for publication.

(38) The total electron distribution used in this sentence must be distinguished from the MO density distribution. The former is the sum of the latter as expressed in eq 6 of paper I. For individual MO's, the statement is not always correct due to the delocalized character of each MO (in extreme case, due to the symmetry restriction on MO).

$\text{LiHLi}^-$ ,  $\text{BeHBe}^+$ , and  $\text{HeHHe}^+$ , to be stable and their structures to be linear and symmetric. In the present ESF theory, the shapes of these ions are easily predicted to be linear, since even if the molecule is slightly bent, no AD force can be grown on the central hydrogen atom because of the lack of the p-type orbitals on hydrogen (central symmetry effect).<sup>42</sup> In order to discuss the stabilities of these ions, the forces acting on the constituent nuclei must be calculated from reliable wavefunctions.<sup>40,41</sup>

Dierksen, *et al.*,<sup>41</sup> Poshusta, *et al.*,<sup>18</sup> and Ray<sup>19</sup> have also performed *ab initio* calculations of  $\text{LiHLi}^+$  and  $\text{HHHe}^+$ , which indicated that these two- and three-valence-electron ions should be stable and linear. Although the above considerations easily predict these ions to be linear, an essential difference between these ions and other two-valence-electron ions like  $\text{HLiH}^+$ ,  $\text{H}_3^+$ , and  $\text{Li}_3^+$  (these ions are triangular<sup>18,19</sup>) is not clear. Since in these ions the concept of "bond" becomes vague, it may be dangerous to image the EC force along the bond (see also the discussions given in the section of  $\text{AH}_2$  molecules). It may be safer to go back to the fundamental equation (eq 1 or 5, paper I).

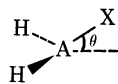
In relation to this section, the structures of  $\text{He}_3^+$  and  $\text{LiHeH}^+$  are interesting, where the central atom is helium instead of hydrogen. Similar considerations as above predict these ions to be linear, since the helium atom also does not have p-type AO's as the hydrogen atom.<sup>42</sup> *Ab initio* calculations predicted these ions to be stable and linear.<sup>18</sup>

**$\text{H}_2\text{AX}$  Molecules and Their Derivatives.** The shapes of  $\text{H}_2\text{AX}$  molecules and their derivatives in the ground and excited states are summarized in Table IV. The

**Table IV.** Shapes of  $\text{H}_2\text{AX}$  Molecules and Their Derivatives

Shape	Occupation No. of MO			$\text{H}_2\text{AX}^a$
	$\pi(\sigma_p)$	$n_\sigma$	$\pi^*(n_{\pi^*})$	
Planar	2	1	0	$\text{H}_2\text{CN}$ , <sup>b</sup> $\text{F}_2\text{BO}$
	2	2	0	$\text{H}_2\text{CO}$ , $\text{HFCO}$ , $(\text{CH}_3)_2\text{CO}$ , <sup>c</sup> $\text{Cl}_2\text{CO}$ , $\text{Cl}_2\text{CS}$
Pyramidal	2	1	1	$\text{H}_2\text{CO}^*$ (31, 35°; $\sim 20^\circ$ ), <sup>d</sup> $\text{HFCO}^*$ ( $\sim 40^\circ$ ), $(\text{CH}_3)_2\text{CO}^*$ , <sup>c</sup> $\text{Cl}_2\text{CS}^*(32^\circ)$
	2	2	1	$\text{H}_2\text{CF}$ ( $< 5^\circ$ ), <sup>e</sup> $\text{H}_2\text{NO}$ (26°) <sup>f</sup>
	2	2	2	$\text{H}_2\text{NCl}$ (69.6°) <sup>g</sup>

<sup>a</sup> The values in parentheses are the out-of-plane angle defined by



The experimental angles are cited from ref 15 except those specially noted. The asterisk means that the molecule is in the  $n_\sigma \rightarrow \pi^*$  excited state. <sup>b</sup> E. L. Cochran, F. J. Adrian, and V. A. Bowers, *J. Chem. Phys.*, **36**, 1938 (1962). <sup>c</sup> C. N. R. Rao, G. C. Chaturvedi, and H. S. Randhawa, *Chem. Phys. Lett.*, **7**, 563 (1970). <sup>d</sup> References 15 and D. E. Freeman and W. Klemperer, *J. Chem. Phys.*, **45**, 52 (1966). <sup>e</sup> Reference 28. <sup>f</sup> Theoretical value: A. W. Salotto and L. Burnelle, *J. Chem. Phys.*, **53**, 333 (1970). <sup>g</sup> Reference 16.

MO density distributions are illustrated in Figure 2 for  $\pi$ ,  $n_\sigma$ ,  $\pi^*$ , and  $\sigma_s^*$  MO's in planar configuration.<sup>36</sup> They are very similar to those of HAX molecules except  $n_\sigma$  MO, which is the in-plane  $p_{\pi^-}$ -type lone-pair

(42) Although small mixing of  $p_{\text{H}}$  AO should occur, the extent is so small that the resultant AD force cannot overcome the restoring force due to the EC force.

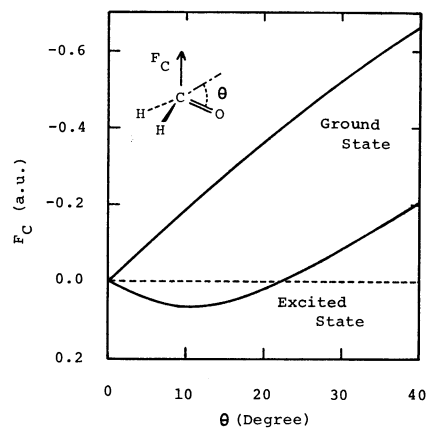


Figure 3. Forces acting on carbon nuclei in the ground and  $n \rightarrow \pi^*$  excited states of  $\text{H}_2\text{CO}$  calculated from the INDO electron distributions.

orbital mainly localized on X atom. This orbital does not contribute to  $D(p_{\pi A})$  and is unimportant for shape.  $\pi^*$  MO becomes  $n_{\pi^*}$  MO in the pyramidal configuration, which is chiefly localized on A atom.

An important difference of  $\text{H}_2\text{AX}$  molecules from HAX molecules lies in the increase of the EC force along one more AH bond. Other things are very similar to those in HAX molecules. Then, the shapes of  $\text{H}_2\text{AX}$  molecules can be discussed along very similar lines to those in HAX molecules. Thus, if the  $\pi^*$  MO is empty, the molecule will be planar, while if the  $\pi$  MO is filled and the  $\pi^*$  MO is singly or doubly filled, the molecule will be pyramidal. A considerable increase in the extent of bending should occur from molecules of singly filled  $\pi^*$  MO to those of doubly filled  $\pi^*$  MO. These predictions agree for all the molecules shown in Table IV. Moreover, if the  $\sigma_s^*$  MO is filled, the molecule will become linear again.

From the above discussions, a similar result to the Walsh rule is obtained for the ground-state  $\text{H}_2\text{AX}$  molecules. If the number of valence electron is less than or equal to 12, the molecule will be planar, while if it is 13–14, the molecule will be pyramidal. A considerable increase in the extent of bending should occur from 13 to 14. If the number of valence electron increases to fill  $\sigma_s^*$  MO (16 or 18), the molecule will become linear again.

For the prototype molecule  $\text{H}_2\text{CO}$ , we plotted in Figure 3 the force acting on the carbon atom for the various out-of-plane angles,  $\theta$ . The method of calculation is the same as that used in drawing Figure 1. In Figure 3, the ground state is calculated to be planar and the  $n \rightarrow \pi^*$  excited state to be pyramidal ( $\theta \simeq 22^\circ$ ). The experimentally known out-of-plane angles of the latter are 31–35°<sup>15</sup> or  $\sim 20^\circ$ .<sup>43</sup> Interestingly, the  $n \rightarrow \pi^*$  excited state of HFCO is more pyramidal ( $\theta \simeq 40^\circ$ ) than that of  $\text{H}_2\text{CO}$  as expected from the inductive effect of fluorine.<sup>13</sup> Similar to  $\text{H}_2\text{CO}$ , the shape of  $(\text{CH}_3)_2\text{CO}$  is planar in its ground state<sup>16</sup> and pyramidal in its  $n \rightarrow \pi^*$  excited state.<sup>44</sup> The experimental out-of-plane angle of the latter is not yet known precisely.<sup>44</sup>

For the  $\pi \rightarrow \pi^*$  excited states of the molecules whose valence-electron number is 10–12, the prediction of

(43) D. E. Freeman and W. Klemperer, *J. Chem. Phys.*, **45**, 52 (1966).

(44) C. N. R. Rao, G. C. Chaturvedi, and H. S. Randhawa, *Chem. Phys. Lett.*, **7**, 563 (1970).

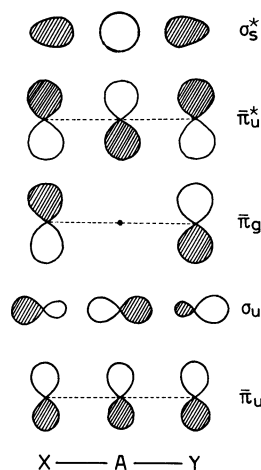


Figure 4. Illustration of the MO density distributions in XAY molecules. A hatch is made in order to show the bonding and antibonding characters of the MO's.

molecular shapes becomes rather difficult, since in these,  $D(p_{\pi A})$  becomes very near to unity.<sup>36</sup> The situation is very similar to the  $\text{CH}_3$  radical. Although the shapes of  $\pi \rightarrow \pi^*$  excited states are expected to be planar, the substituent effect and the central atom effect will considerably affect the shapes. At present, no firm experimental evidences are known for this prediction.

A comparison between the molecular shapes of  $\text{H}_2\text{CO}$  and  $\text{H}_2\text{COH}$  is interesting. The  $\pi$ -inductive effects of oxygen atoms in these two molecules are reverse to each other; that in  $\text{H}_2\text{CO}$  is  $\pi$  attractive and that in  $\text{H}_2\text{COH}$  is  $\pi$  donating. Therefore, although  $\text{H}_2\text{CO}$  is planar,  $\text{H}_2\text{COH}$  is nonplanar.<sup>37</sup> The role of the OH substituent in going from  $\text{CH}_3$  to  $\text{H}_2\text{COH}$  is very similar to that of the F substituent in  $\text{H}_2\text{CF}$ <sup>28</sup> discussed in detail in paper I. Dobbs, *et al.*,<sup>45</sup> showed from esr measurements that the degree of bending increases from mono oxygen-substituted radicals (*e.g.*,  $\text{H}_2\text{COH}$ ,  $(\text{CH}_3)_2\text{COH}$ ) to bis oxygen-substituted radicals (*e.g.*,  $\text{HC}(\text{OCH}_2)_2\text{O}$ ,  $\text{CH}_3\text{C}(\text{OCHCH}_3)_2\text{O}$ , etc.).

**XAY Molecules.** In order to predict the shapes of XAY molecules in their ground and excited states, the knowledge of MO density distribution in linear structure is very useful as in the previous sections. They are illustrated in Figure 4.  $\bar{\pi}_u$ ,  $\bar{\pi}_g$ , and  $\bar{\pi}_u^*$  MO's<sup>17</sup> are the bonding, nonbonding, and antibonding orbitals composed of three  $p_{\bar{\pi}}$  AO's centered on the A, X, and Y atoms. Among these, only  $\bar{\pi}_u$  and  $\bar{\pi}_u^*$  MO's contribute to  $D(p_{\bar{\pi}A})$ .  $\bar{\pi}_u^*$  MO makes a larger contribution than  $\bar{\pi}_u$  MO, due to the bonding and antibonding effects discussed in the section on HAX molecules.<sup>36</sup> There are other,  $\pi_u$ ,  $\pi_g$ , and  $\pi_u^*$ , MO's which are perpendicular to these MO's. Although these MO's do not contribute to  $D(p_{\bar{\pi}A})$ , they affect the EC force through bonding and antibonding effects.<sup>36</sup> The  $\sigma_u$  MO between  $\pi_u$  ( $\bar{\pi}_u$ ) and  $\pi_g$  ( $\bar{\pi}_g$ ) MO's is composed of three  $p_{\sigma}$ -type AO's centered on A, X, and Y atoms. The  $\sigma_s^*$  MO is an  $s_A$ - $\sigma_X$  and  $s_A$ - $\sigma_Y$  antibonding orbital.

As seen from Figure 4, when the  $\bar{\pi}_u^*$  MO is empty,  $D(p_{\bar{\pi}A})$  is considerably less than unity, since even if the  $\bar{\pi}_u$  MO is filled,  $D(p_{\bar{\pi}A})$  is smaller than or nearly

(45) A. J. Dobbs, B. C. Gilbert, R. O. C. Norman, *Chem. Commun.*, 1353 (1969).

equal to two-thirds (two electrons are spread over three  $p_{\bar{\pi}}$  AO's). Then, in this case, the molecule should be linear. However, when the electron(s) begin(s) to fill  $\bar{\pi}_u^*$  MO owing to the increase in electron number or to the excitation of electron from  $\pi_g$  ( $\bar{\pi}_g$ ) or  $\sigma_u$  MO's below,  $D(p_{\bar{\pi}A})$  becomes larger than unity. Then, the molecule should become bent. Moreover, a considerable decrease in apex angle should occur from  $(\bar{\pi}_u^*)^1$  to  $(\bar{\pi}_u^*)^2$ . On the other hand, when  $\sigma_s^*$  MO is filled, no important AD force can be grown on atom A in  $\pi$  and  $\bar{\pi}$  directions due to the central symmetry effect. Therefore, the molecule should become linear again.

The shapes of XAY molecules in their ground and excited states are summarized in Table V. There is

Table V. Shapes of XAY Molecules

Geometry and electronic configuration <sup>a</sup>	XAY <sup>b</sup>
Linear ( $\pi_u$ ) <sup>2</sup> ( $\sigma_u$ ) <sup>0</sup>	OLi <sub>2</sub> <sup>c</sup>
Linear ( $\pi_u$ ) <sup>4</sup> ( $\sigma_u$ ) <sup>m</sup> ( $\pi_g$ ) <sup>n</sup> $m \leq 2$ $n \leq 4$	C <sub>3</sub> (2, 0), C <sub>3</sub> * <sup>(1, 1)</sup> ; CCSi(2, 0), CCSi* <sup>(1, 1)</sup> ; CCN(2, 1), CCN* <sup>(1, 2)</sup> ; CNC(2, 1), CNC* <sup>(1, 2)</sup> ; NCN(2, 2), NCN* <sup>(1, 3)</sup> ; BO <sub>2</sub> (2, 3), BO <sub>2</sub> * <sup>(1, 4)</sup> ; NCO(2, 3), NCO* <sup>(1, 4)</sup> ; CO <sub>2</sub> <sup>+</sup> (2, 3), CO <sub>2</sub> <sup>+</sup> * <sup>(1, 4)</sup> ; OCS <sup>+</sup> (2, 3), OCS <sup>+</sup> * <sup>(1, 4)</sup> ; CS <sub>2</sub> <sup>+</sup> (2, 3), CS <sub>2</sub> <sup>+</sup> * <sup>(1, 4)</sup> ; N <sub>3</sub> (2, 3), N <sub>3</sub> * <sup>(1, 4)</sup> ; NNO <sup>+</sup> (2, 3), NNO <sup>+</sup> * <sup>(1, 4)</sup> ; NNO(2, 3)
Linear ground ( $\pi_g$ ) <sup>4</sup> ( $\pi_u^*$ ) <sup>0</sup>	CO <sub>2</sub> , CS <sub>2</sub> , NCO <sup>-</sup> , NCS <sup>-</sup> , N <sub>3</sub> <sup>-</sup> , OCS, NNO, NO <sub>2</sub> <sup>+</sup>
Bent excited ( $\pi_g$ ) <sup>3</sup> ( $\pi_u^*$ ) <sup>1</sup>	CO <sub>2</sub> * <sup>(122°)</sup> , CS <sub>2</sub> * <sup>(135.8°)</sup> , NCO <sup>-</sup> * <sup>(...)</sup> , NCS <sup>-</sup> * <sup>(...)</sup> , N <sub>3</sub> <sup>-</sup> * <sup>(...)</sup>
Bent ( $\pi_g$ ) <sup>m</sup> ( $\pi_u^*$ ) <sup>n</sup> $3 \leq m \leq 4$ $1 \leq n \leq 4$	NO <sub>2</sub> (4, 1, 134.1°), NO <sub>2</sub> * <sup>(3, 2, 121°)</sup> ; <sup>d</sup> CF <sub>2</sub> (4, 2, ...), CF <sub>2</sub> * <sup>(3, 3, ...)</sup> ; SiF <sub>2</sub> (4, 2, 101°), SiF <sub>2</sub> * <sup>(3, 3, ...)</sup> ; NO <sub>2</sub> <sup>-</sup> (4, 2, 115.4°), NO <sub>2</sub> <sup>-</sup> * <sup>(3, 3, ...)</sup> ; ONF <sup>(1, 4, 2, 110°)</sup> , ONF* <sup>(3, 3, ...)</sup> ; SO <sub>2</sub> (4, 2, 119.5°), SO <sub>2</sub> * <sup>(3, 3, 126.1°)</sup> ; SSO(4, 2, 118°), SSO* <sup>(3, 3, ...)</sup> ; ONCl(4, 2, 116°), ONBr(4, 2, 117°), O <sub>3</sub> (4, 2, 116.8°), NF <sub>2</sub> (4, 3, 104.2°), ClO <sub>2</sub> (4, 3, 117.6°), OF <sub>2</sub> (4, 4, 103.8°), OCl <sub>2</sub> (4, 4, 110.8°), SCl <sub>2</sub> (4, 4, 101°), TeBr <sub>2</sub> (4, 4, ~98°), ClO <sub>2</sub> <sup>-</sup> (4, 4, 110.5°)
Linear ( $\pi_u$ ) <sup>4</sup> ( $\sigma_s^*$ ) <sup>2</sup>	IBrCl <sup>-</sup> , Br <sub>3</sub> <sup>-</sup> , ICl <sub>2</sub> <sup>-</sup> , ClIBr <sup>-</sup> ; IBr <sub>2</sub> <sup>-</sup> , I <sub>3</sub> <sup>-</sup> , XeF <sub>2</sub> <sup>g</sup>

<sup>a</sup> The MO density distributions are illustrated in Figure 4. Both  $\pi$  and  $\bar{\pi}$  MO's are written as  $\pi$ . <sup>b</sup> Values in parentheses are  $m$ ,  $n$ , and experimental apex angles, which are cited from ref 15 and 16 except those specially noted. The asterisk means that the molecule is in the excited state. <sup>c</sup> From *ab initio* SCF calculations; see ref 24. <sup>d</sup> The structure of the Rydberg excited state of NO<sub>2</sub>, ( $\pi_g$ )<sup>4</sup>( $\pi_u^*$ )<sup>0</sup>( $3p_{\sigma}$ )<sup>1</sup> is linear. <sup>e</sup> R. C. L. Mooney, *Phys. Rev.*, **47**, 807 (1935); *Z. Krist., Sect. A*, **98**, 324 (1938); *ibid.*, **100**, 519 (1939). <sup>f</sup> R. M. Bozorth and L. Pauling, *J. Amer. Chem. Soc.*, **47**, 1561 (1925). <sup>g</sup> S. Reichman and F. Schreiner, *J. Chem. Phys.*, **51**, 2355 (1969); P. Tsao, C. C. Cobb, and H. H. Classen, *ibid.*, **54**, 5247 (1971).

no exception missing from the above predictions. Since all of these molecules have filled  $\bar{\pi}_u$  MO, their shapes can be grouped with respect to the occupation number of  $\bar{\pi}_u^*$  MO, so long as the  $\sigma_s^*$  MO is empty: if it is zero, the apex angle is 180°; if it is unity, the apex angle is 122–136° (mean value, 131°); and if it is 2–4, the apex angle is 100–126° (mean value, 112°). Interestingly, OLi<sub>2</sub> is easily expected to be linear from the above discussions. (See the section of AH<sub>2</sub> molecules.) For the Rydberg excited state of NO<sub>2</sub>, ( $\pi_g$ )<sup>4</sup>( $\pi_u$ )<sup>0</sup>( $3p_{\sigma}$ )<sup>1</sup>, the shape is expected to be the same as that of NO<sub>2</sub><sup>+</sup>, namely to be linear, since an electron



in the  $3p_z$  orbital exerts no force on the nitrogen atom from symmetry.

The above discussions mean that the shapes of XAY molecules are connected with the number of valence electrons. If it is less than or equal to 16, the molecule should be linear, and if it is 17–20, the molecule should be bent. From 17 to 18, the apex angle should considerably decrease. If the number of valence electron is 22, the molecule should be linear again. These results agree with the Walsh rule.<sup>1</sup>

Among XAY molecules, there are exceptions for which the shapes cannot be understood only from the number of valence electrons. They are the geometries of alkaline-earth dihalides, which we discuss in the next section.

**Geometries of Alkaline-Earth Dihalides.** The geometries of alkaline-earth dihalides have been examined by many theories of molecule structure,<sup>5,7,46</sup> since in this case, the geometry depends upon the metal–halogen combination; *i.e.*, the linear form is favored by the light metal–heavy halogen combination, whereas the bent form is favored by the heavy metal–light halogen combination. Table VI summarizes the observed

**Table VI.** Geometries of Alkaline-Earth Dihalides<sup>a</sup>

Central metal	Halogen			
	F (4.0)	Cl (3.0)	Br (2.8)	I (2.5)
Be (1.5)	l	l	l	l
Mg (1.2)	l	l	l	l
Ca (1.0)	b	l	l	l
Sr (1.0)	b	b	l	l
Ba (0.9)	b	b	b	b

<sup>a</sup> l, linear; b, bent (ref 47). Values in parentheses are Pauling's electronegativities (ref 48).

geometries.<sup>47</sup> Since the original Walsh diagram<sup>1</sup> predicted these geometries to be all linear, Hayes<sup>46</sup> has modified it considering the influences due to the normally unoccupied d orbitals of the metal atoms and succeeded in explaining the observed trends in geometries. Bartell<sup>5</sup> has suggested that the VSEPR theory might not be a good tool to account for the observed geometries, although some reasonings might be possible in the framework of this theory. Pearson<sup>7</sup> has suggested the possibility that MO orderings might be different between the linear and bent molecules.

In the present ESF theory, the observed trends in geometries shown in Table VI can be explained without assuming the roles of d orbitals, the changes in MO orderings, etc. In Table VI, the values given in parentheses are the Pauling's electronegativities.<sup>48</sup> By

(46) E. F. Hayes, *J. Phys. Chem.*, **70**, 3740 (1966).

(47) L. Wharton, R. A. Berg, and W. Klemperer, *J. Chem. Phys.*, **39**, 2023 (1963); A. Büchler, J. L. Stauffer, W. Klemperer, and L. Wharton, *ibid.*, **39**, 2299 (1963); A. Büchler, J. L. Stauffer, and W. Klemperer, *ibid.*, **40**, 3471 (1964); *J. Amer. Chem. Soc.*, **86**, 4544 (1964).

(48) L. Pauling, "The Nature of Chemical Bond," 3rd ed, Cornell University Press, Ithaca, N. Y., 1960.

changing halogens from I to F, the  $\sigma$ - and  $\pi$ -inductive effects become respectively more attractive and donating. Then, the AD force acting on the metal increases. Moreover, from the central atom effect, this AD force is expected to increase rapidly by changing the central metal from Mg to Ca (see Figure 3 of paper I). Similarly, the EC force decreases by changing halogens from I to F and by changing central metals from Be to Ba. The attractive GC force between the negative gross charge on halogen and the other positive halogen nucleus increases in the same order as the EC forces decrease. To sum up, since all three kinds of forces prefer the bent structure in the order of halogens from I to F and of metals from Be to Ba, the observed trends in geometries shown in Table VI are understandable. Moreover, the first appearance of the bent structure in  $\text{CaF}_2$  is reasonable as a consequence of rapid increase in the AD force from Mg to Ca.

### Concluding Remarks

In the present paper, the ESF theory developed in paper I has been applied to the shapes of a wide variety of molecules of the types  $\text{AH}_2$ ,  $\text{AH}_3$ ,  $\text{HAX}$ ,  $\text{XHY}$ ,  $\text{H}_2\text{AX}$ , and  $\text{XAY}$  in their ground and excited states. Since the roles and the relative importances of the AD, EC, and GC forces in determining the shapes of molecules were clarified in paper I, we had only to consider the magnitudes and changes of these forces from molecule to molecule and from state to state. For this purpose, we used simple MO density distributions in relation to Figure 7 of paper I and the substituent effects, central atom effect, central symmetry effect, etc. From these, the ESF theory has been proved to be very successful in predicting the shapes of both the ground and excited states of a large number of molecules belonging to the above types. Indeed, among these molecules for which the shapes are known experimentally, no exceptions were found missing from the theory. Moreover, the present theory was shown very useful in understanding not only the trends within a type of molecule but also the relations among different types of molecules. Similar to the Walsh rule,<sup>1</sup> the ESF theory also correlates shapes of molecules with the number of valence electrons, although the basic approach is quite different. Especially, the present theory gave very simple and clear accounts even to the shapes of the molecules for which other theories of molecular structure such as the Walsh rule, the VSEPR theory, and the SOJT theory found difficult to give straightforward explanations ( $\text{Li}_2\text{O}$ , alkali hydroxides, alkaline-earth dihalides, etc.).

**Acknowledgment.** The author wishes to acknowledge Professors Teijiro Yonezawa and Hiroshi Kato for encouragement and valuable discussions. He also thanks the members of Quantum Chemistry Group of his department for useful discussions.